Summary Report on Phase 1 Feasibility Study of In-Drift Diffusion

Qinhong (Max) Hu, Timothy Kneafsey, and Joseph S.Y. Wang

Lawrence Berkeley National Laboratory

Jeff Roberts and Steve Carlson

Lawrence Livermore National Laboratory

This report summarizes the work performed and findings obtained during the Phase 1 (feasibility study) of the Engineered Barrier System (EBS) in-drift diffusion evaluation. The objective of this work is to characterize and reduce uncertainties associated with measurements of diffusion coefficients and modeling of diffusion processes. Phase 1 of the study evaluates measurement and modeling uncertainties as well as scoping alternative measurement and modeling approaches. Phase 2 of the study consists of rigorous diffusion testing of invert materials (employing approaches developed from Phase 1) and the development of a calibrated invert diffusion model (with separate surface and internal water components if needed to interpret measured diffusion data) for use in total system performance assessment (TSPA).

The invert between the waste package/drip shield and the tuff host rock is integral to both the EBS and the Unsaturated Zone (UZ) performance, and is important to the TSPA dose calculation. TSPA for Site Recommendation (TSPA-SR) and Repository Safety Strategy Revision 4 (RSS-4) identify diffusion in the invert as a major transport mechanism. An invert diffusion barrier (slow radionuclide diffusion through the invert), if effective, can greatly enhance waste-isolation capacity. The diffusion data set reported by Conca and Wright (1992) is generally well correlated in terms of a power-dependence on the volumetric water content. This "universal" or "fully correlated" power function has been used to represent diffusive transport of radionuclides through the invert in TSPA-SR (CRWMS M&O, 2000), without taking into consideration any unique properties of specific invert materials. Crushed porous rock may provide unique characteristics that vary greatly from this generic power function (Wang et al., 2001; Hu and Wang, 2001). For example, Conca (1990) has inferred the existence of very low diffusion coefficient in tuff gravel samples with modest water content, orders of magnitude lower than the values derived from the generic power function. Porous tuff gravel samples were placed in a high relative humidity

chamber (RH) not in contact with fluid sources. At equilibrium, all samples were observed to become surface air dry in a nearly 100% humidity atmosphere and no electrical conductivity could be measured. This resulted in an inferred diffusion coefficient below 10^{-15} m^2/s, which is Conca's detection limit (using electrical conductivity [EC] measurements for estimating the diffusion coefficient). Equilibrium water content of the tuff gravel samples has a fairly large value of 2.7%. The inferred low diffusion value of 10^{-15} m^2/s at this water content deviates significantly from the TSPA-SR data-set diffusion coefficient (about 2.8×10^{-12} m^2/s) obtained with continuous fluid introduction. In other words, at the same total water content, diffusion in samples prepared within the high-humidity experiment (without fluid source contact) is almost three orders of magnitude lower than the samples prepared with liquid-water introduction (contact). Water distributions among surface and internal porespace in porous gravel lead to such unique diffusion behavior. Small pores and the relatively large porosity of tuff gravel could play an important role in retaining water in the internal pores, reducing the surface water content of the gravel to levels where diffusion becomes as low as the detection limits of conventional methods. This diffusion behavior needs further evaluation to fully substantiate the invert diffusion barrier concept.

The scope of the feasibility study includes the following activities: (1) review of the literature on diffusion data to determine if the universal function (diffusion coefficient as a function of bulk water content) used by TSPA-SR properly represents the diffusion behavior of porous gravel; (2) evaluation/verification of the electrical conductivity/Nernst-Einstein method to infer diffusion coefficients used in TSPA-SR; and (3) development of other direct approaches to diffusion measurement (e.g., microscale profiling of diffusing tracers distribution). The work was conducted under applicable QA requirements, and documented in Scientific Notebooks YMP-LBNL-JSW-QH-1E (pages 91-147), YMP-LBNL-JSW-QH-2 (pages 1-63), YMP-LBNL-JSW-TJK-1 (pages 1-97), and LLNL-SCI-4G2-VI (pages 1-18).

Status and Findings

1. Literature Review:

A thorough literature review has been conducted and the results have been submitted to a peer-reviewed journal (*Critical Reviews in Environmental Science and Technology*) for potential publication (Hu and Wang, 2001). A presentation was also made in the International High-Level

Radioactive Waste Management Conference held in April, 2001, which provided a good forum for focused discussions of the potential for the invert barrier to improve the performance of the potential geologic repository (Wang et al., 2001).

In summary, we have reviewed the behavior of, and relationship between, nonsorbing diffusion species and water content, particularly for porous aggregates (e.g., rock gravel). At low moisture contents, aqueous diffusion is postulated to occur in thin liquid films on the gravel surfaces, and the diffusion will be very slow if the water film is discontinuous. Diffusion is monotonically related to water content, but the relationship is not simple and depends upon the range of water content (e.g., different forms of relationships at different water-content ranges). The literature data further show that the relationship is related to the texture of the geologic medium. Figure 1 (from Hu and Wang, 2001) presents the relationship, based on data compiled from the literature, between diffusivity ratio (ratio of effective diffusion coefficient D_e to aqueous diffusion coefficient D_0) and the water content for media with different textures. The relationship appears to be related to potential energy status or mobility of water, rather than just the magnitude of water content. The location of the curve is related to the texture, with coarse-textured media to the left and fine-textured media to the right. If these curves are extrapolated to $D_e/D_0=0$, the critical (or threshold) water content (q_c, when the diffusion coefficient approaches zero or the detection limit of the measurement method) decreases as texture becomes more coarse. The finer the texture, the higher the q_c values, because a larger amount of water exists in fine-textured media than in coarse-textured media at similar water-potential energy. Rowell et al. (1967) reported the q_c value to be 0.13 for a sandy loam soil. Below this q_c, the continuity of the liquid phase is thought to break down, and the viscosity of the liquid next to the soil particles increases significantly (Rowell et al., 1967).

Porous-rock gravel exhibits unique water distribution characteristics. Rock surfaces in partially saturated environments will generally be wetted by liquid films that can be held either by adsorptive forces on mineral surfaces or by capillary effects in surface roughness. For a porous-rock-gravel system, the total water content is comprised of surface water (including surface film water around grains and pendular water between rock grain contacts) and internal water (water contained within the rock matrix pores). This internal water is not likely to contribute significantly to water flow and transport in the unsaturated gravel system (Conca and Wright,

1990). Pendular water elements between gravel grains serve as the bridging pathways between grains and control the efficiency of the system in attaining the upper limit of transport determined by surface films. Diffusion in rock gravel could be very slow, because water films on surfaces can be discontinuous or absent. Conca and Wright (1992) reported an experimental method to determine diffusion coefficients (using the Nernst-Einstein equation) by using an unsaturated-flow apparatus in combination with electrical-conductivity measurements. However, experimental limitations may exist in this approach, such as the contact resistance at low water contact and the applicability of the Nernst-Einstein equation in geologic media at very low saturation. To further explore the low diffusion potential in unsaturated porous gravel, it has been determined that refinement of available testing methods or the development of innovative approaches to diffusion methods is needed.

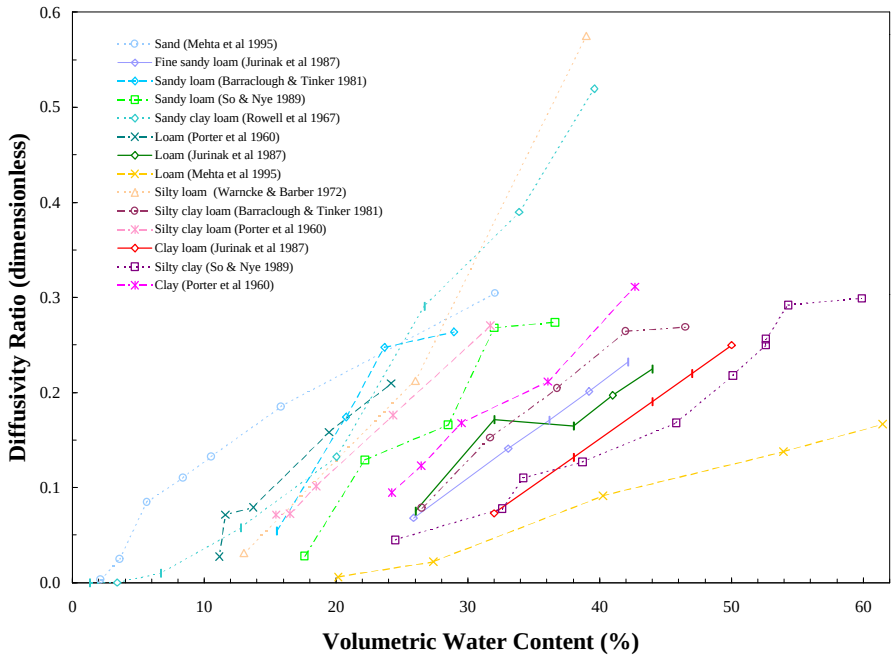

Figure 1. Compilation from the literature on diffusion data as a function of water content, showing the effect of medium texture on diffusion and critical water content (from Hu and Wang, 2001).

Hu and Wang (2001) also compiled available models in the literature that describe the relationship between diffusion coefficient and water content. Some models include parameters related to medium properties, such as water retention that is in turn related to pore-size distribution. A two-part model relation to account for the critical water content was also presented by Fityus et al. (1999) and Olesen et al. (1999). Olesen et al. (1999) introduced a diffusivity model (Equation 1) that incorporated a soil-water-retention parameter, b.

$$D_e/D_0 = 0.45\, q\, (q - 0.022b)\ /\ (f - 0.022b), \quad q \geq 0.022b \qquad (1a)$$

$$D_e/D_0 = 0, \qquad q < 0.022b \qquad (1b)$$

In Equation 1, q is the water content and f is the porosity. Parameter b (>0) corresponds to the slope of the soil-water characteristic curve in a log-log plot, which is a simple and convenient measure of the pore-size distribution of the soil. The value of $0.022b$ in Equation 1 equals the q_c of continuous water films. Olesen et al. (1996) reported an approximately linear correlation between the q_c and parameter b. The reported water content of 2.7% from Conca's (1990) RH experiments is likely the q_c value for the tested tuff gravel.

In summary, diffusion in unsaturated geologic media is not solely dependent upon the magnitude of water content. It is rather related to the mobility of water. In porous rock gravel, appreciable water can exist inside the internal pores, without significantly contributing to the overall diffusion. On the other hand, the surface water, though minor relative to the internal water, can control the connectivity of diffusion pathways and diffusion in porous gravel.

2. Laboratory Testing:

2.1. Preparation of Rock Samples

Tuff samples (SPC 527451) from the middle nonlithophysal zone of the Topopah Spring Tuff were collected, crushed, and sieved into various size fractions. The sieves used for size separation were calibrated by a Yucca Mountain Project-approved contractor. Tuff samples were also machined into a cubic shape to be used in the diffusion evaluation, using a micro-profiling approach (Section 2.3).

2.2. Diffusion Measurements by the Electrical-Conductivity Method

2.2.1. Introduction:

This work was mainly conducted at LBNL in collaboration with LLNL scientists regarding test design, instrumentation, fabrication, implementation, data collection, and data interpretation. The work intends to evaluate/validate the electrical conductivity measurements that constitute the TSPA-SR diffusion data set.

As discussed above, diffusion of radionuclides in unsaturated gravel could occur very slowly on the solid mineral surface, through water in the interconnected porosity (present within the gravel grains) or through water films (present on the gravel surfaces). Previous research has indicated that diffusion through the water films is the most important mechanism (Conca and Wright, 1990). Measuring low diffusion coefficients requires long duration measurements, the ability to sample on extremely small spatial scales, or an indirect approach. Calculating diffusion coefficients based on the electrical conductivity measurements is an indirect technique that has been accepted for diffusants in bulk aqueous samples (Conca and Wright, 1992). The Nernst-Einstein equation relates the electrical conductivity of a solution to the diffusivity ($D = \frac{RT}{F^2}\frac{qGt_i}{Z_i C_i}$).

Here, R is the universal gas constant (8.314 J/K mol), T is the absolute temperature, F is Faraday's constant (96485.309 C/mol), q is the geometric factor of the experimental cell, G is the conductance, t_i is the transference number, Z_i is the valence of the diffusant, and C_i is the diffusant molar concentration.

If we consider the connected aqueous film in an unsaturated porous medium as the only electrical-current-carrying pathway (assuming the conductivity of the mineral and open porespace is negligible), we can measure a resistivity and calculate a diffusivity. This method directly accounts for the tortuosity of the fluid pathway on the gravel surface and the diffusion resistance at intergranular contacts.

Extending the application of the Nernst-Einstein equation to diffusion in unsaturated porous media requires several assumptions. We first must assume that the water films are thick enough

to act as bulk water. However, nearest the mineral surface, the water molecules will be relatively fixed (unlike bulk water). Ions opposite in charge to the surface charge will be concentrated near the surface, while similarly charged ions will be repelled from the surface. In very thin water films, both of these layers will be compressed towards the mineral surface. Although they may be significant, in this work, we have ignored any effects of this water structure.

Here, we have measured the resistance of crushed tuff occupying a cell with known dimensions. The tuff has been preconditioned with preset water contents, and the water contains a known concentration of potassium chloride. Using the measured resistance and known geometry, we have calculated diffusion coefficients. We have plotted these against the volumetric water content and compared them to measurements made by others.

2.2.2. Method

A cell was constructed to contain tuff gravel, isolate the sample from the atmosphere, and apply four electrodes (Figure 2). The cell was constructed out of transparent PVC pipe with inside diameter of 6.225 cm. Nylon endcaps were machined such that two O-rings were placed between each endcap and the PVC pipe, and each endcap was fitted with a stainless-steel electrode to make contact with the sample across the entire cross-sectional area of the pipe. Two stainless-steel screen electrodes were placed in the center of the cell approximately 65 mm apart. A sealable access port was placed between the two screen electrodes.

The crushed tuff used in the measurements was from the 2-4 mm fraction of tuff sample with porosity and bulk density of 10.5% and 2.234 g/cm^3 respectively. The grains were shard-like, often with one dimension greater than 4 mm. The tuff was somewhat friable, and grain breakage was observed during normal laboratory handling.

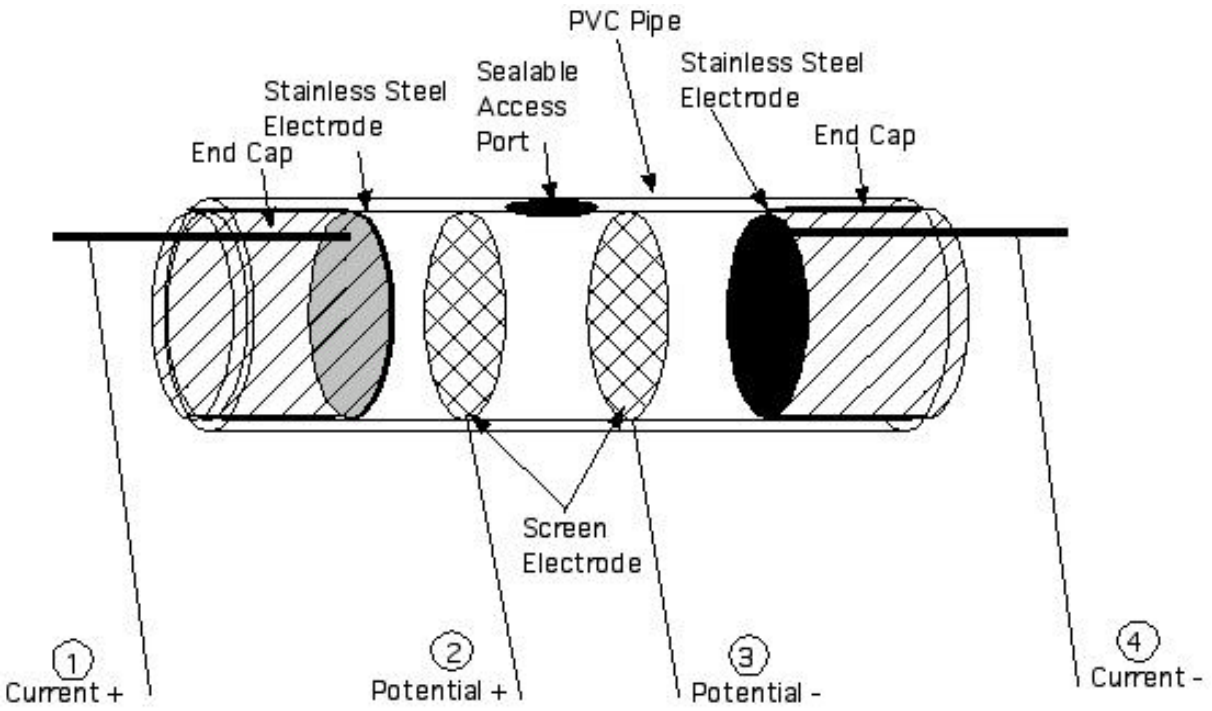

Figure 2. Measurement cell.

The crushed tuff was vacuum saturated in 0.5 g/L KCl solution. The three compartments of the cell were filled with crushed tuff at the desired volumetric water content, ranging from cell saturation to less than 5%. Tuff was compacted into each of the cell compartments, and the porosity of each of the three compartments was assumed to be equal. High water contents were initially used (saturated and initial drainage), and these were attained by simply emplacing the saturated tuff in the cell with the saturating brine (0.5 g/L KCl) and draining the sample, using a porous ceramic drain in the cell. Further tuff drainage was accomplished using an ultracentrifuge. Portions of the saturated tuff were placed in centrifuge cups and drained under specified conditions. Following the centrifugation, the tuff was placed into the cell inside a glove bag maintained at high relative humidity by a beaker of warm water. This was to prevent dryout of the surface layer of water on the tuff grains. After filling the cell, the cell was placed into an incubator maintained at 22 ^{o}C for several hours to allow for thermal equilibration.

Resistance measurements were made using a GenRad 1692 Digibridge LCR meter. The calibrated Digibridge was checked against many resistance measurement systems and found

reliable for the expected conditions. Prior to making measurements, the Digibridge was zeroed according to the manufacturer's instructions. The four electrodes from the cell were connected to the four ports of the meter, and resistance (series) was recorded for the five frequencies generated by the meter (100 Hz, 120 Hz, 1000 Hz, 10,000 Hz, and 100,000 Hz). For measurements with high water contents, measurements were made primarily at 1000 Hz, as the quality factor (Q) indicated by the meter was low. Q provides an indication of the phase shift (Q=tan(phase shift)) between the current and voltage measurement. The Nernst-Einstein equation requires the passive resistance (phase shift=0), thus the resistance value for the frequency with the lowest Q was selected for diffusion coefficient calculation. In many cases, alternate electrode configurations were connected to the meter and the resistance was recorded. Using the electrode numbers from Figure 2, we made measurements for some water contents in the 1144, 1122, 2233, 3344, 1234 [four electrode], 1133, and 2244 configurations, where 1144 indicates that Current+ was connected to electrode 1, Potential+ to electrode 1, Potential- to electrode 4, and Current- to electrode 4. Because both positive connections were connected to one electrode and both negative connections were connected to another electrode, we call this a two-electrode measurement. This allowed for an analysis of two- and four- electrode measurement techniques.

2.2.3. Results

The diffusivities calculated using the Nernst-Einstein equation for volumetric moisture content are shown in Figure 3 and Table 1. The five points with volumetric water content greater than 5.4% were attained by drainage of the initially brine saturated cell. Volumetric water contents below 5.4% were achieved by centrifuging vacuum-saturated tuff at 1000, 2000, 3000, 4000, and 8000 rpm in a Beckman L8-60M/P HT ultracentrifuge prior to placing it in the cell. The tuff appeared drier and drier as the centrifuge speed increased. Any handling of the tuff resulted in some breakage. Centrifugation at 8,000 rpm resulted in a high amount of smaller particles being generated (and a higher packing density in the cell).

2.2.4. Discussion

The calculated diffusion coefficients were compared to those presented by Conca and Wright (1990) and to the data presented in DTN MO9807SPA00026.000 (Figure 3). The diffusion coefficients measured here are consistent with previously reported values. In our measurements,

we had difficulty reducing the volumetric water content below 5% (on a cell volume basis). The volumetric water content declined only slightly on a tuff grain basis as the centrifuge speed was increased, resulting in increased drainage. These changes resulted in increases in measured resistance and decreases in the calculated diffusion coefficient, without any apparent decrease in volumetric water (content the cell basis).

Using the centrifuge at high speed fragmented the tuff. The reduction in grain size had multiple effects. First, it caused a higher packing density resulting in a larger volumetric water content. Secondly, it enlarged the surface area, thereby increasing the current pathways and the number of intergrain contacts. These factors decreased the measured resistance, providing a higher diffusion coefficient.

As mentioned previously, an important aspect of the use of the Nernst-Einstein equation is that the mode of electrical conduction must be known. That is, to use the Nernst-Einstein equation to calculate diffusion coefficients in an aqueous system, there must be an understanding of the contribution to total electrical conduction from various possible modes of current conduction. If other modes of current conduction are present (such as through the mineral, on the dry mineral surface, through adsorbed water on the mineral surface, through the intragranular pore space, or at the grain/grain connections), the Nernst-Einstein equation may not be applicable or these individual effects may require quantification. It has been shown that at low saturations, densely welded tuff has a significant surface conduction contribution to total electrical conduction (Roberts and Lin, 1997).

Table 1. Diffusion coefficients and cell conditions during measurements.

Tuff grain volumetric water content (cm^3/cm^3)*	0.945	0.194	0.118	0.118	0.118	0.114	0.104	0.103	0.097	0.098
Cell volumetric water content**	0.547	0.092	0.055	0.055	0.055	0.052	0.050	0.052	0.049	0.050
Intergranular Porosity	0.494	0.494	0.494	0.494	0.494	0.539	0.517	0.495	0.494	0.487
D_{avg} (cm^2/s)	6.53E-06	3.46E-07	1.39E-07	1.48E-07	1.36E-07	5.27E-08	2.22E-08	2.03E-08	2.00E-08	1.24E-08

* Calculated volumetric water content based on the crushed tuff bulk volume (=volume of water/total volume of tuff grains including intragranular porosity). Values exceeding the grain porosity (0.105) indicate conditions beyond grain saturation.

** Calculated volumetric water content based on the cell volume (=volume of water/cell volume)

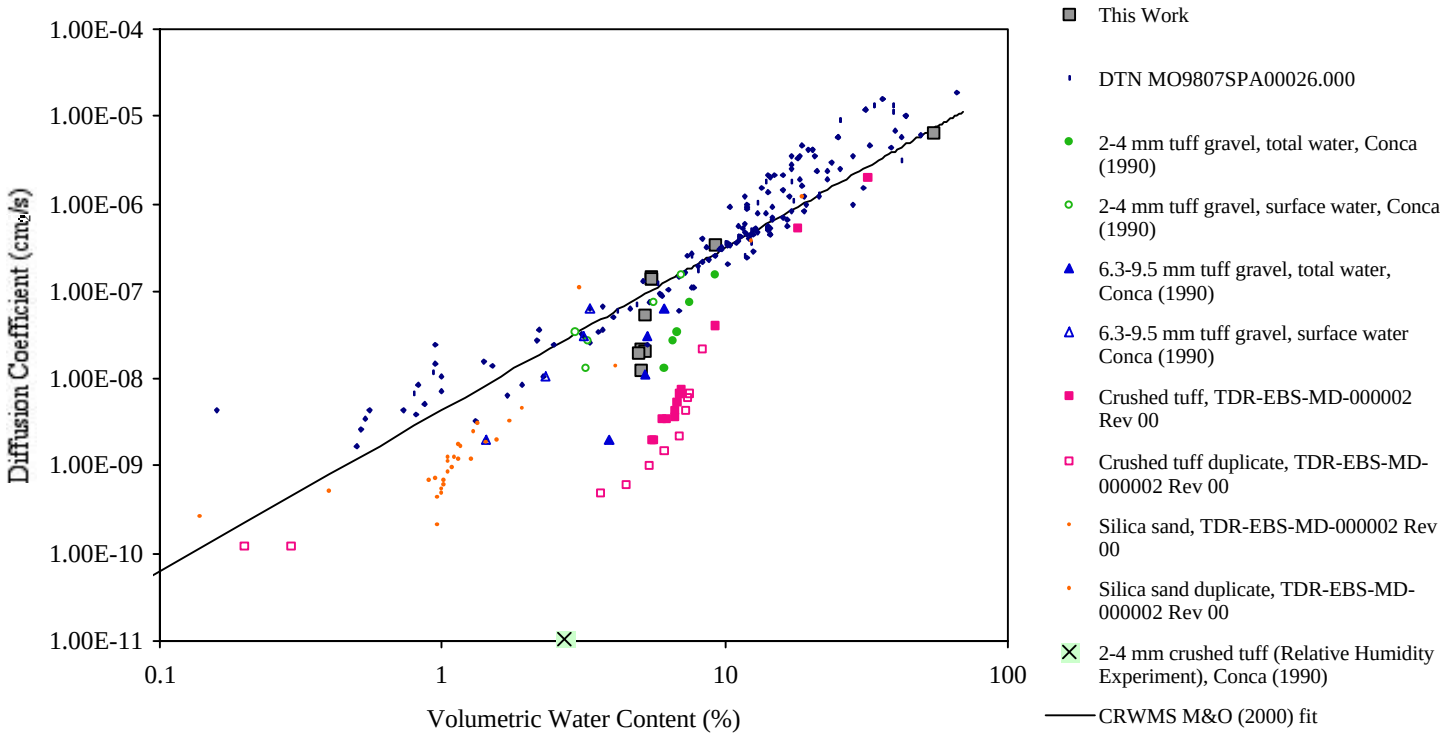

Figure 3. Diffusion coefficient versus volumetric water content for this and other work.

Other concerns include electrode design, electrode/sample polarization, and contact impedance at the electrode/sample interfaces. These problems can be minimized by constructing optimally sized and shaped sample holders and by performing experiments on samples in which electrode spacing is the only variable. We have attempted to assess the effects of electrode-contact impedance during this feasibility study by making measurements with a four-electrode configuration and multiple two-electrode configurations. When a four-electrode configuration is used, current is applied across the outer electrodes and potential is measured across the inner electrodes. In the wires and electrodes, current is carried by electrons; in the water-rock system, current is carried by ions. This change in charge carrier from electronic to ionic occurring at the current electrode/rock interface results in contact impedance. The inner electrodes measure only the potential, and very little current is drawn from the system to make this measurement, thus there is no contact impedance at these electrodes. Calculating the resistance between the potential electrodes can then be accomplished without the influence of contact impedance. Using the two-electrode configuration, current is applied and potential is measured at the same two electrodes. Thus, any contact impedance is included in the resistance calculation. This contact impedance was minimal at high volumetric water contents, but increased to as much as 5% of the indicated resistance in the drier measurements.

An additional problem with electrode-sample contact is that for the Nernst-Einstein equation to apply we needed a passive resistance (near-zero phase angle). As the sample water content changed, the frequency providing the most passive resistance (smallest phase angle) also changed. For most of the two electrode measurements, 1000 Hz was the best of the five frequencies available on the GenRad 1692. For the four electrode measurements, 100 and 120 Hz provided more passive resistances.

The geometry of the measurement cell also affected the phase shift. Values of Q close to zero were obtained across a wider frequency range (1,000 Hz–10,000 Hz) for the two electrode measurements across the entire cell, whereas for the shorter intervals, frequencies near 1,000 Hz were required.

It is possible that additional conduction mechanisms (indeed the ones of interest) may be obscured by electrode contact impedance or would not be observed over the limited frequencies of the present test. The four-electrode configuration is designed to reduce electrode contact impedance, but might not be adequate for extremely resistive samples. A different electrode geometry and measurement frequency may improve the accuracy of these measurements.

It is appropriate to ask what the effects of grain size and internal porosity are. The effect of grain size has not been adequately investigated. All of our specimens had nominally the same grain size. Much larger volumes would be necessary for larger gravel sizes. With these larger grain sizes, it would be difficult to establish the appropriate moisture conditions and representatively measure both resistance and physical properties to the accuracy needed. An ultracentrifuge might limit preparation to three grains at a time, and the use of relative humidity chambers would require the very slow transfer of large amounts of mass. Under similar thermodynamic conditions, smaller grains provide larger surfaces. If we assume that the surface film controls the electrical conduction (and thus the diffusivity), smaller grains should provide less diffusive resistance. Further investigation is needed to verify this.

The effect of internal porosity also requires further study. Nonconnected internal porosity (isolated pores) will not impact steady state diffusion, but will provide a reservoir for sorption of radionuclides, extending the duration of transient diffusive transport.

If the surface film controls diffusive transport, the film itself requires better characterization. This cannot be accomplished by gravimetric analysis for porous gravel because the mass of the surface-held film is too small compared to the mass of water held within the intragranular pore space. From our analysis, we were not able to state what portion of the water was present inside or outside the tuff grains. A comparison of diffusion on porous and nonporous minerals with similar roughness (and under similar thermodynamic conditions) would help in answering this question. Alternative approaches, such as studying grain-boundary migration rates in the presence of thin films, might aid in the assessment of diffusion at such low saturation conditions (i.e., Nakashima, 1995).

2.3. Diffusion Measurements by Micro-Profiling Method

Laser ablation refers to the process in which an intense burst of energy delivered by a short laser pulse is used to vaporize a minute sample (in the range of nanograms) from a specific location. The chemical composition of the vaporized sample is then analyzed with inductively coupled plasma-mass spectrometry (ICP-MS). Laser ablation, coupled with ICP-MS (LA-ICP-MS), has recently evolved as a powerful analytical tool for solid samples (Russo et al., 2000). LA-ICP-MS can determine simultaneously a large number of chemical elements with very low detection limits. The high spatial resolution (in the range of microns) achieved by a focused laser beam makes LA-ICP-MS a very attractive investigative approach for slow diffusion processes. This section describes the method development, diffusion test design, and obtained preliminary diffusion results using LA-ICP-MS.

2.3.1. Development of LA-ICP-MS Method

A detailed study was conducted to evaluate the potential of the LA-ICP-MS approach to direct measurement of diffusion coefficients, both at rock surfaces and within rock matrix. This study included choosing appropriate tracers, probing elements intrinsic to tuff that can serve as internal standards to correct for different LA-ICP-MS conditions, evaluating surface profiling (moving the sampling point to the next location along the surface) and depth profiling (sampling deeper depths at the same location), and examining crater depths from certain laser pulses. Figure 4 shows the relationship between the signal responses for nine elements intrinsic to tuff as a function of the number of laser pulses. Intensity in the y-axis indicates the signal (counts per second, cps) measured by ICP-MS (VG-PQ3 Spectrometer) from the laser-abated mass. Figure 4 shows that the response is linear up to about 100 laser pulses, corresponding to a depth of about 135 µm. Beyond that depth, the laser is out of focus.

Laser focusing can be adjusted in the laser system (CETAC LSX-200 Laser Ablation System). Figure 5 presents a surface profile of a tuff sample with rough surfaces for the same nine elements conducted by sampling every 1.5 mm. To do this, we adjusted the laser focus as indicated from the laser ablation system. The stable responses for these intrinsic tuff elements indicate that we sampled nearly the same volumes at each location, which increases our confidence of representative solid sampling (even for rough surfaces).

The CETAC laser ablation system can also let the user choose among several available spot sizes available (from 25 µm to 200 µm) allowing choice of the appropriate spot size for different applications. A smaller spot size will, under the same number of laser pulses, sample less solid material, leading to lower analytical precision. Additionally, since smaller spot size on the rock is sampled, more heterogeneity will be observed. The tuff consists largely (~99 vol. %) of the former glassy matrix now devitrified to fine crystals of cristobalite, alkali feldspar, and quartz of 3-10 µm size fractions, as shown from the scanning electron microscopy analysis (Johnson et al., 1998). A combination of spot size and number of laser pulses could be made to meet different research objectives. For example, tens of laser pulses can be fired at a 25 µm spot size for surface profiling if the diffusion distance is on the order of less than a millimeter. Alternatively, a 100 µm spot size can be used for depth sampling with several laser pulses applied consecutively at a sampling location.

Table 2 presents responses of intrinsic tuff elements from laser ablation. Peterman and Cloke (2001) reported a very uniform distribution of elemental compositions in tuff. Our data reflect the trend observed in the reported elemental compositions; percent weight level for Al and K, trace (parts per million) level for Ce and Th. Relative response (concentration divided by signal) is related to the atomic number of the elements, with heavier elements showing a higher sensitivity to ICP-MS. Evaluation from many tests indicates that Al consistently exhibits the best signal stability (i.e., least heterogeneity) among all the intrinsic tuff elements. We could, therefore, use the ratio approach (dividing the response of the element of interest [the tracer chemical in this case] to the response of Al) to provide a normalized response that corrects any uncertainty related to LA-ICP-MS. This uncertainty could include, for example, less mass abated as the sampling depth increases. The normalization would, in this case, differentiate the reduced signal caused by the reduced mass from the small concentration of the tracer. Normalization for surface profiling is not required, whether the surface is rough (after focus adjustment, shown in Table 2), machined, or machined and polished, because the relative standard deviation (RSD) does not show much improvement between normalized and non-normalized approaches.

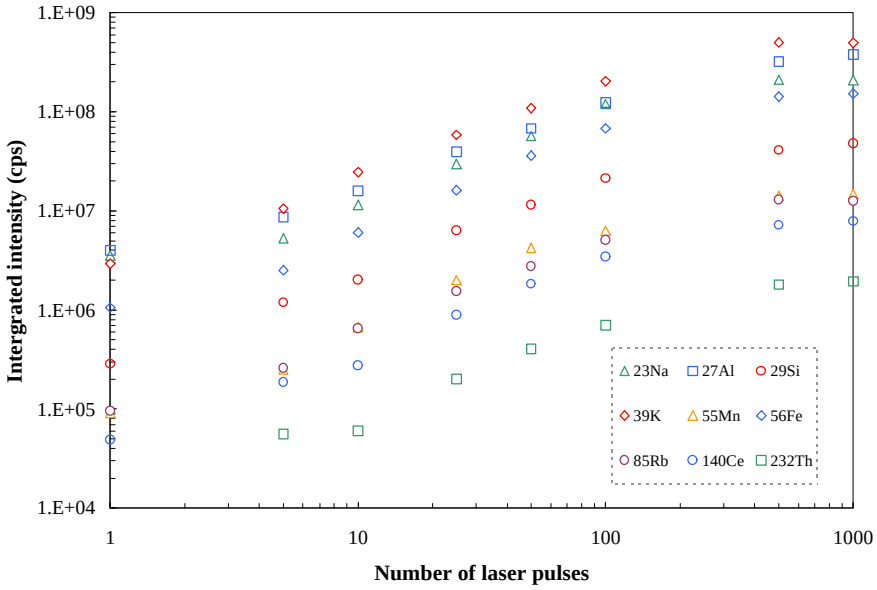

Figure 4. Linearity between responses of intrinsic tuff elements and numbers of laser pulses at a nominal 100 µm spot size.

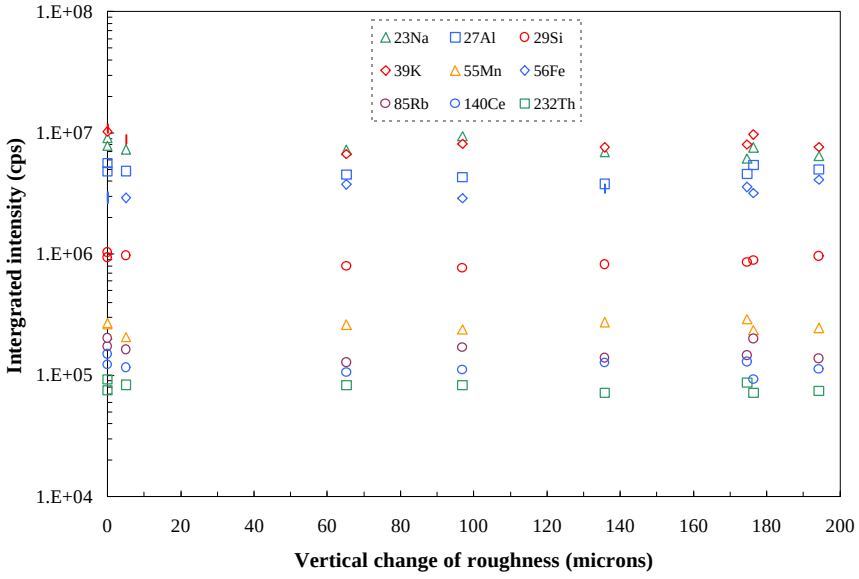

Figure 5. Surface profiling of a tuff sample with a rough surface (100 µm spot size, 20 laser pulses).

Figure 6 shows the crater shape and depth from laser ablation on tuff. The results indicate that the obtained spot size of the crater is consistent with the spot size chosen from the laser system. Furthermore, although the crater has a quite smooth bottom after 50 laser pulses, rougher profiles are obtained with fewer laser pulses, as expected. Crater depth is proportional to the number of laser pulses applied. This information provides us with confidence in correlating the number of laser pulses to the crater depth, i.e., the sampling distance (during depth profiling) of tracer distribution for diffusion evaluation in rock matrix.

2.3.2. Diffusion evaluation

A half-cell approach was used to prepare samples for diffusion evaluation using the LA-ICP-MS sampling and measurement technique. In this approach, an element (e.g., a tuff cube in this work) containing a tracer was placed in contact with an element not containing the tracer, both under the same thermodynamic conditions. The tracer will then diffuse from the tracer-containing element to the other. Machined 1.5 cm tuff cubes were used in this feasibility study. Tracers were chosen based on their chemical similarity to radionuclides of interest. The source tuff cube (Figure 7) was vacuum-saturated with a tracer solution that contained a mixture of NaBr, $NaReO_4$, CsBr, and RbBr. Both Br^- and perrhenate (ReO_4^-) act as nonsorbing tracers. Perrhenate serves as an analog to technetium, which exists in a form of pertechnetate ($^{99}TcO_4^-$). Cesium (Cs^+) and rubidium (Rb^+) were used as cationic tracers to examine the delayed diffusive transport from chemical sorption and retardation. Nonradioactive Cs was used as a surrogate for radioactive ^{137}Cs. The sink tuff cube was also vacuum-saturated, but without tracers. Source and sink cubes were then separately placed inside a humidity chamber within an incubator maintained at 22^{o}C. The high (near 100%) relative humidity was maintained by the evaporation from free-standing water beakers inside the enclosed chamber. Cube weight was monitored over time until it reached a constant weight after 13 days. This pre-equilibration is to ensure an establishment of similar water potential between source and sink cubes to prevent/minimize potential advection process. The cubes were then clamped together and left in the RH chamber to start the diffusion test.

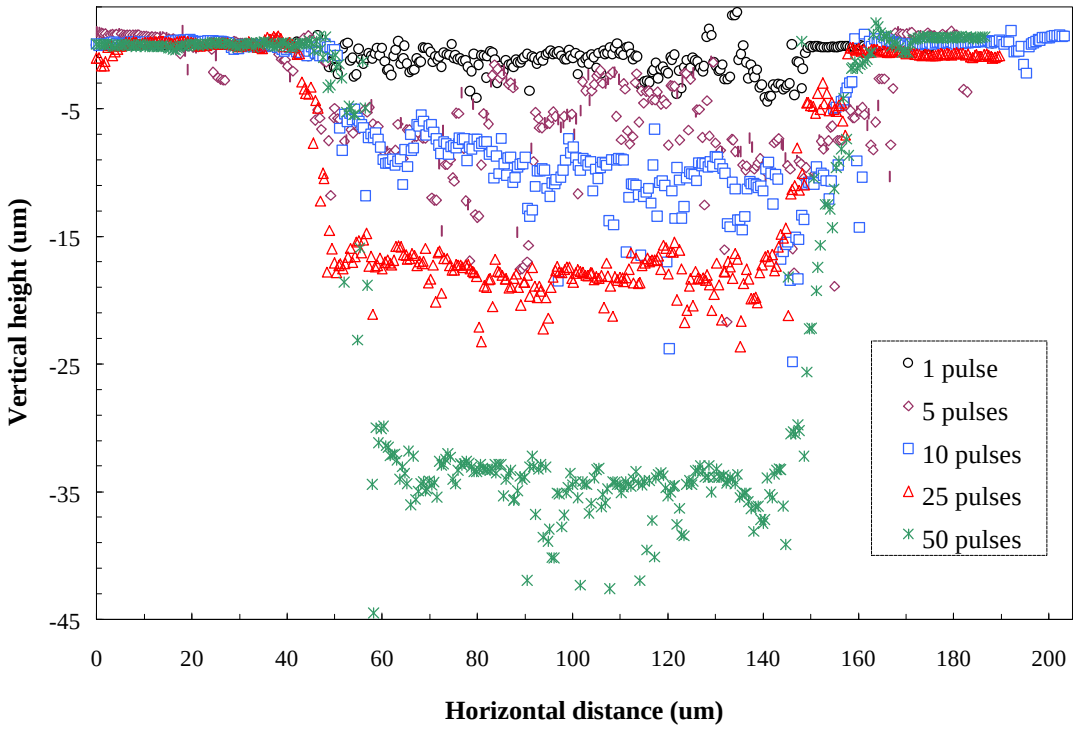

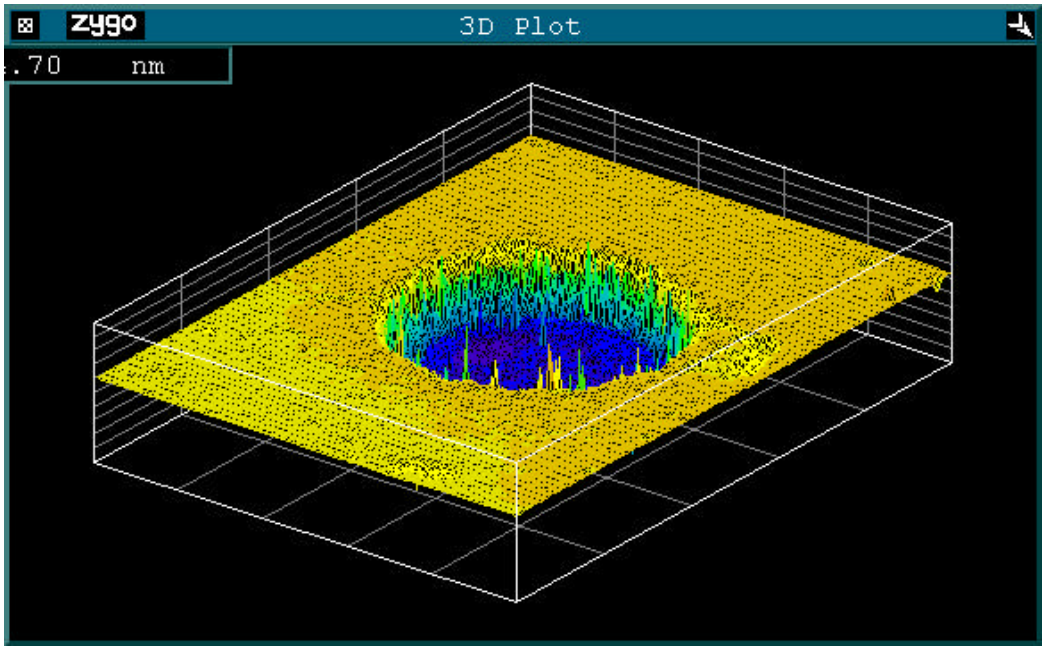

Figure 6. Crater depth and shape at a nominal 100 µm spot size. (A) Surface profiles at different laser pulses. (B) 3-D plot for 50 laser pulses.

Table 2. Results from analysis of a tuff sample with rough surfaces (100 μm spot size; 20 laser pulses; a total of 9 data points)

Element	^{23}Na	^{27}Al	^{29}Si	^{39}K	^{55}Mn	^{56}Fe	^{85}Rb	^{140}Ce	^{232}Th
Concentration (ppm) *	26,113	66,421	356,604	40,096	526.6	7795	186.8	77.4	26.0
Mean response (counts per second, cps)	7549,853	4,773,558	893,209	8,641,412	254,524	3,304,594	162,227	118,526	80,166
Relative response (cps/ppm)	289.1	71.9	2.5	215.5	483.3	423.9	868.5	1,531.7	3,086.0
Relative Standard Deviation (%)	14.6	11.7	10.0	16.0	9.7	13.4	16.7	13.6	9.0

* from Peterman and Cloke (2001).

After 87 days, the diffusion test was stopped by separating the interface connection of source and sink cubes. The surface and depth tracer distribution was then mapped (Figure 7), using LA-ICP-MS. Figure 8 shows the tracer distribution and comparison for both the source and sink cubes. Nonsorbing tracers (ReO_4^- and Br^-) are evidently present almost entirely across the sink cube face (Face 3) that is perpendicular to the interface face (i.e., in the direction of surface diffusion), which indicates rapid diffusion (to be calculated later). Sorbing tracers (Cs^+ and Rb^+) travel about 10 mm from the interface face as a result of their sorption onto the tuff matrix. (This behavior was also observed from the results obtained for other faces, as well as another diffusion test with a diffusion time of 150 days.) Tracer distribution is corroborated from the results on the far-side face of the sink cube, where nonsorbing tracers are detected while sorbing tracers are nearly at background levels. As expected, the tracer distributions on the far-side face of the source cube are more uniform, as well as at much higher concentrations than the diffusion faces. Furthermore, the interface side has a similar tracer concentration distribution for both the source and sink cubes.

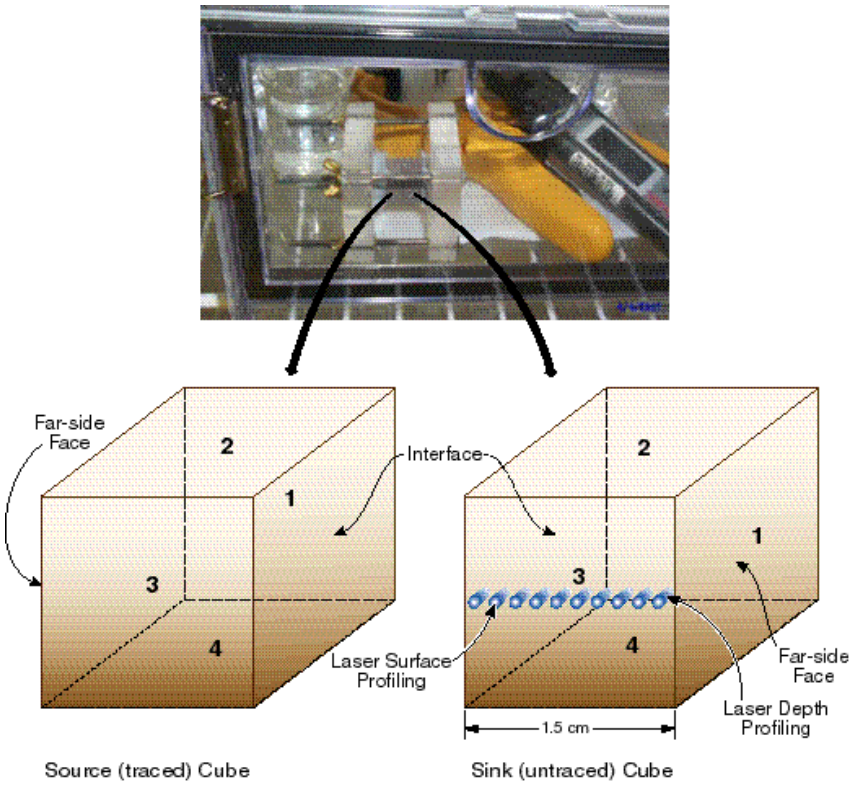

Figure 7. Half-cell diffusion experimental setup and schematics of surface and depth profiling. Face designation is also indicated.

Note that responses for Br^- and Rb^+ distribution are not as good as those for ReO_4^- and Cs^+, because of the low sensitivity of bromide analysis to ICP-MS and the moderate abundance of rubidium in tuff (187 ppm, as reported from Peterman and Cloke, 2001). Nevertheless, the trend is consistent among both nonsorbing and sorbing tracers. Additional tracers will be used in future work. Furthermore, the edge effect (unusually low concentration at several millimeters distance from the cube edge near the far-side face) is noticed. The cause is not yet clear, but it may possibly be related to the thin Teflon sheet used on the two far-side faces. The Teflon sheet serves as a nonwetting barrier to aqueous diffusion in the half-cell diffusion setup.

Laser profiling was also conducted depth-wise for the sink cube on Face 3 (Figure 9). It is evident that tracer distribution decreases dramatically as the sampling depth increases (on the scale of microns). The results clearly indicate very slow diffusion inside the tuff matrix.

We used the one-dimensional analytical solution (Equation 2) to calculate the diffusion distance into semi-infinite media with a constant source (Crank, 1995):

$$C(x,t) = C_0 \text{ erfc } \{x/[2(D_e \acute{} \, t)^{0.5}]\} \qquad (2)$$

where $C(x,t)$ (M L^{-3}) is the observed concentration based on an initial concentration C_0 (M L^{-3}), x (L) is the distance from the inlet boundary into the medium, t (T) is the time, and D_e (L^2 T^{-1}) is the effective diffusion coefficient of the diffusant in the medium. Because of unsaturated conditions, we expected that the nonsorbing tracers such as ReO_4^- would be diffusively transported more slowly than in bulk aqueous solutions. Because of the somewhat linear profiles observed, however, we were only able to bound diffusion coefficients for the conditions investigated. (In future work, we will determine an actual value of the diffusion coefficient by reducing the diffusion time.) If we use the TcO_4^- aqueous diffusion coefficient for ReO_4^- with a value of 1.48×10^{-9} m^2/s (Sawatsky and Oscarson, 1991), about 92% of the source concentration will exist at a distance of 1.5 cm (our cube side distance) by diffusion after 87 days. This extent of diffusion is observed in surface profiling (with the sampling depth about 9 μm). In other words, the nonsorbing tracer ReO_4^- diffused through the surface water film at a rate similar to its aqueous

diffusion in bulk water. This is not surprising, considering that the tuff cubes (with a measured surface roughness about 2.5 μm) were located in the high RH chamber, with the likely presence of a thick water film that behaves like bulk water. The half-cell is comprised of a cube-cube connection that maximizes source-sink contact. A similar range of water film thickness is observed for glass and natural rock samples. Tokunaga et al. (2000) reported the measured average film thickness on a roughened glass (with a surface roughness of about 9 μm) was kPa and –1.2kPa, which correspond to relative humidities exceeding 99.9% (according to the Kelvin equation). Tokunaga and Wan (1997) also reported that an average surface film thickness on a Bishop Tuff fracture surface with a roughness ~50 μm ranged from 2 to 70 μm at matrix potential greater (more positive) than about –250 Pa (with corresponding RH >99.999%).

To evaluate internal diffusion from the depth profile results, we converted the measured signal to a form of C/C_0 by treating the first depth measurement (2 laser pulses with a depth about 4 μm) as the source concentration for each tracer. This conversion was conducted for all available depth profiling results. Figure 10 indicates that the internal diffusion coefficient for nonsorbing tracers is in the range of 10^{-16} m^2/s, which is nearly seven orders of magnitude lower than that of surface diffusion. This estimation is based on the assumption of a constant tracer source, which is the first 4 μm of the rock surface (in this case). However, the surface concentration is changing, and this assumption is not necessarily satisfied. Nevertheless, the assumption may not be important, since no clear difference is observed among the data (Figure 10), i.e., the depth profile near the interface (60 μm away) does not show a higher internal diffusion than the location farther (410 μm) away. This slow-diffusion- coefficient range is obtained from this preliminary work, and further measurements and analyses are necessary.

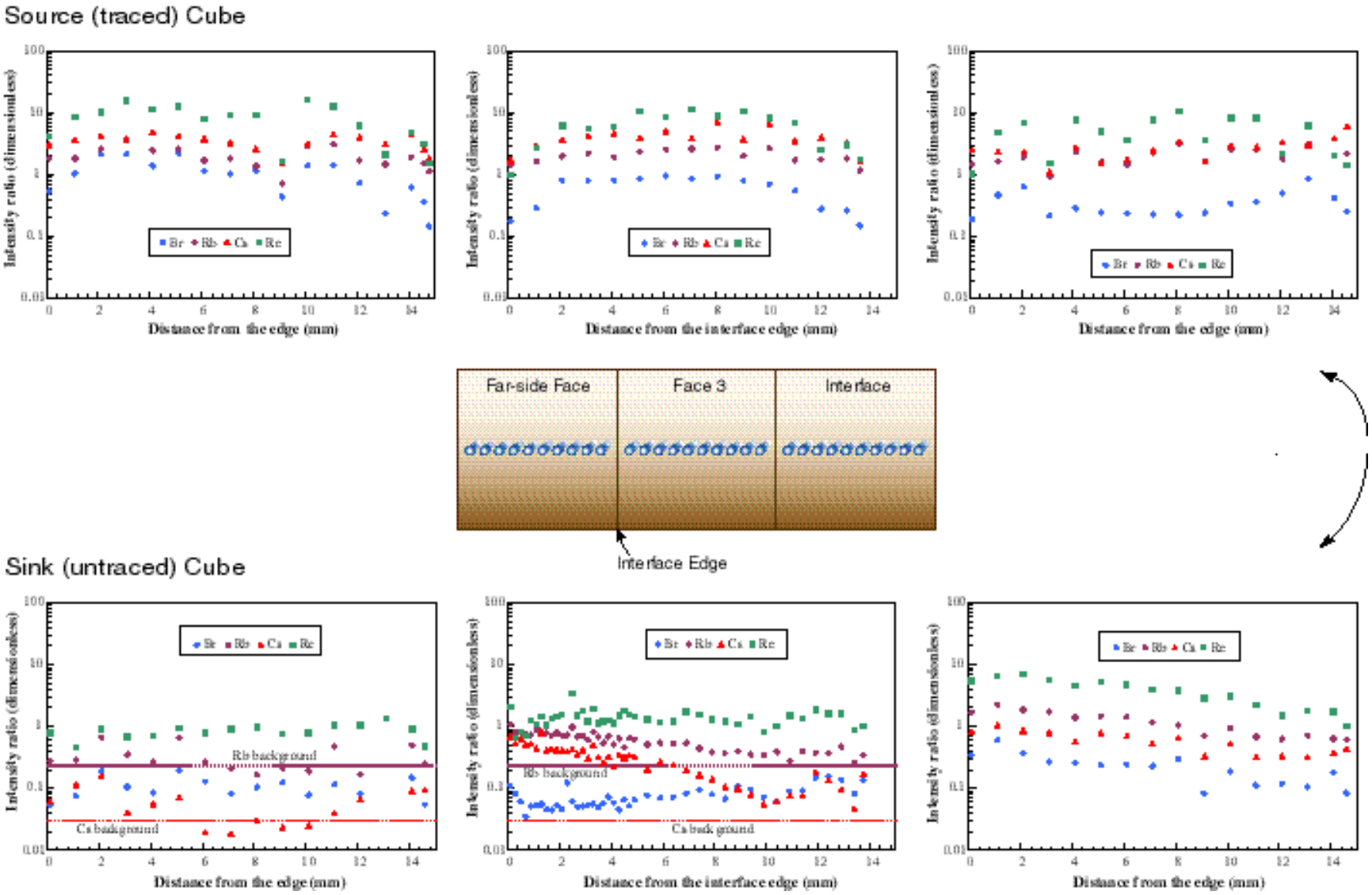

Figure 8. Tracer distribution from surface profiling using LA-ICP-MS (100 µm spot size and 10 laser pulses). Y-axis: intensity ratio denotes the signal of each tracer divided by the signal of aluminum.

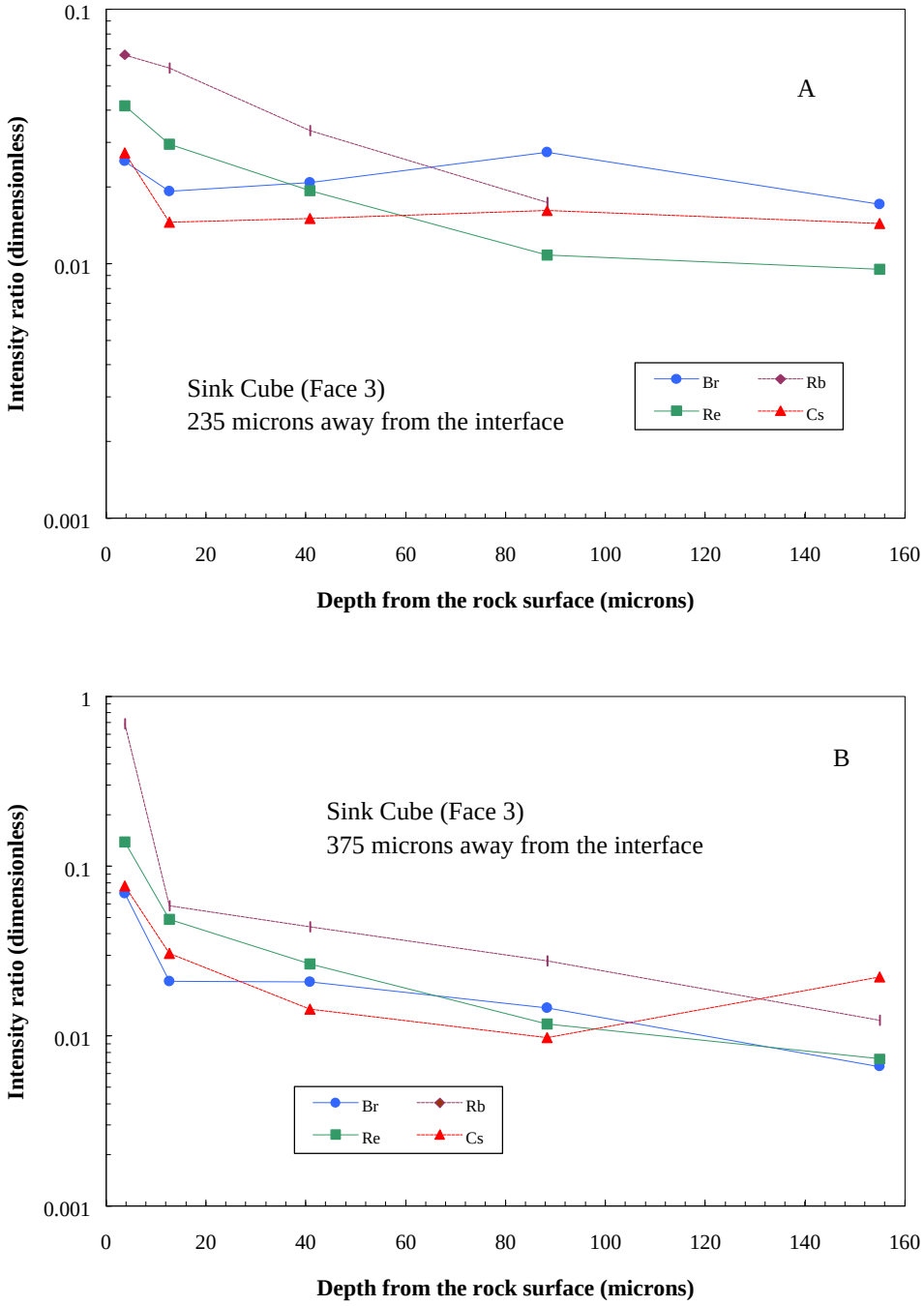

Figure 9. Depth profiling of tracer distribution on Face 3, using LA-ICP-MS (25 µm spot size), at (A) 235 µm, and (B) 375 µm lateral distance away from the interface edge.

The diffusion of Br^- is observed to be relatively faster than ReO_4^-, as expected from its larger aqueous diffusion coefficient (2.08×10^{-9} m^2/s, Cussler, 1984). The molecule of ReO_4^- is larger than Br^-, which can lead to enhanced steric hindrance within narrow tuff pores. Triay et al. (1997) also reported a slower diffusion for TcO_4^- than tritiated water in saturated tuff. The extremely slow internal diffusion indicates the extreme hindrance of diffusion inside tuff matrix under unsaturated conditions, with the measured volumetric grain water content of 8.9% (or equivalent water saturation value of 85.6%). The internal diffusion could be composed of pore-water diffusion (diffusion in relatively large, interconnected water-filled pores and microcracks), grain-boundary diffusion (aqueous diffusion through relatively small pore spaces such as grain boundaries), or intracrystalline diffusion in minerals. Grain boundaries usually contain thin water films on their surfaces. Grain-boundary diffusion through thin intragranular water films in well-consolidated rocks is often much slower than pore-water diffusion because the structure of the thin water film may be more constrained from interaction with solids than "free" water in pores. From compiled literature data for many types of rock, Nakashima (1995) reported that grain-boundary diffusion is less than 10^{-15} m^2/s, and the ratio of pore-water to grain-boundary diffusion is on the order of 100 to 1,000. Kozaki et al. (2001) reported that grain-boundary diffusion was the predominant diffusion process, even for anions like chloride, in saturated montmorillonite. Intracrystalline diffusion will be even slower because of the extremely constricted diffusion through narrow channels within the crystal structure. Rundberg (1987) estimated, from kinetic sorption data, that intracrystalline diffusion coefficients ranged from 1.1×10^{-19} to 6.7×10^{-17} m^2/s for cesium, strontium, and barium in a partially welded devitrified tuff from the Prow Pass unit. This diffusion coefficient also includes sorption effect as the measured sorption distribution for these cations range between about 20–200 ml/g.

Conclusions

We have achieved the feasibility-study objectives of the EBS in-drift diffusion work. We have evaluated use of the electrical conductivity and the Nernst-Einstein equation to measure the diffusion coefficient, and have measured the diffusion coefficient of potassium chloride in 2–4 mm tuff gravel. Our measurements are similar to those made by others; however, we measured steadily decreasing diffusion coefficients with very little decrease in volumetric water content. We have also established a mature and rigorous method of microscale diffusion profiling (with a

spatial resolution on the order of tens of microns for surface profiling and a few microns for depth profiling) to directly measure diffusant tracer distribution. The preliminary results from this microscale diffusion profiling work provide direct evidence and measurement of the surface and internal diffusion.

Unsaturated porous tuff gravel could serve as a unique diffusion and transport barrier because of their water-distribution characteristics. Within relatively low RH environments such as following the heating phase and post-emplacement equilibration period to ambient conditions, surface water films are expected to be discontinuous or completely removed. Diffusive transport of radionuclides in such systems will be greatly reduced. Porous tuff gravel can, however, hold a considerable amount of internal water because of capillary force. They can imbibe liquid from seepage or breached waste packages to minimize drainage of radionuclides through the invert. We conclude, *from the current investigations*, that the unique capacity of unsaturated gravel can be harnessed to maximize the performance of the potential repository. Crushed tuff seems to be an appropriate candidate as the potential invert material from the perspective of diffusion and transport barrier.

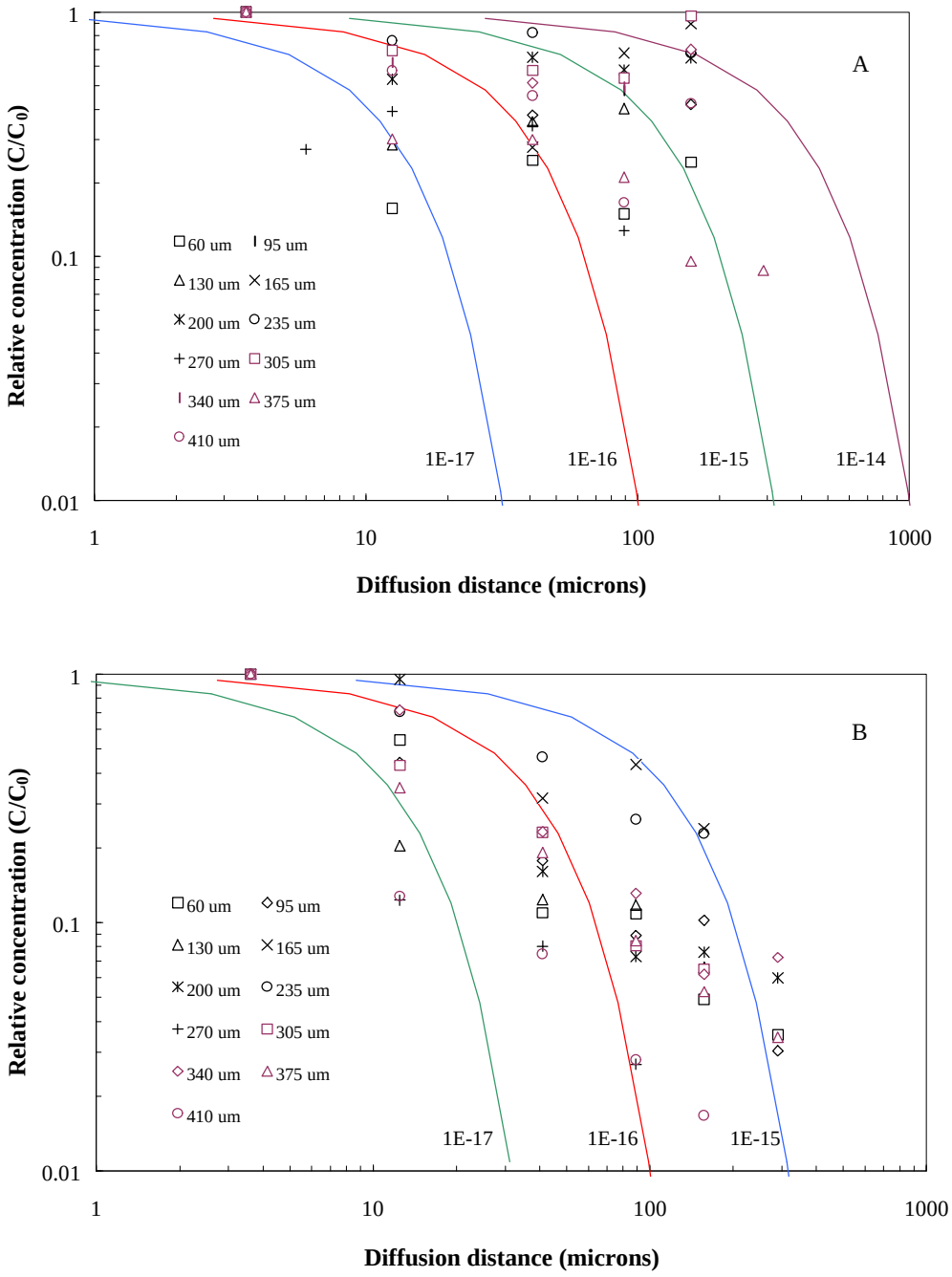

Figure 10. Tracer distribution with respect to different lateral location from the interface (distances shown in the legend): (A) bromide; (B) perrhenate. Solid lines are obtained from 1-D analytical solution to diffusion (Equation 2), with the respective diffusion coefficients (m^2/s) presented on the plot.

Proposed Work for Phase 2 Study

1. Evaluation of various potential invert materials:

   A variety of rock types shall be collected and processed for evaluation as potential invert materials in emplacement drifts. The samples may include the lower lithophysal tuff, granite, and dolostone. Relatively nonporous granite with an internal porosity as low as 0.5% will provide a strong contrast to the porous tuff (10% porosity). This difference will provide a good comparison with regard to the contribution of internal and surface water components to chemical transport from diffusion and/or advective drainage. Additionally, the thermal history of a mineral affects its sorptive properties (hydrophobicity), with heat-treated quartz samples being more hydrophobic than nonheat-treated samples (Gee et al., 1990). This thermal effect could impact diffusion through a gravel invert. To maximize the performance of invert materials in the potential repository, we need to systematically consider the different characteristics of invert materials. These characteristics could include physical properties, such as matrix porosity (large porosity is conductive to liquid retention in the case of seepage to a small/moderate extent), wettability (affecting surface water film thickness and continuity in different RH conditions), geochemical compatibility with the host rock, mechanical stability to support the waste packages, chemical reactivity with radionuclides, and availability.

   Different-sized fractions of invert materials are to be tested as to their diffusion behavior. Choice and size of invert materials will be coordinated with the EBS design group to ensure compatible and consistent design approaches, including design requirements for the invert to carry heavy loads and any thermally related performance criteria ascribed to the invert.

2. Full-scale diffusion measurements:

   2A. Electrical conductivity approach: this is a continuing collaborative effort between LBNL and LLNL. Work will be expanded to quantify the effects of very thin water films coating grains, grain size, and internal porosity on diffusion. Testing with low-porosity granite and heat-treated quartz will enable us to examine much lower (total) water contents than possible for the more porous tuff and will also provide necessary information on thermal effects or useful treatment technologies for gravel pretreatment.

2B. Microscale diffusion profiling using LA-ICP-MS: This is a continuing effort at LBNL. The work will be expanded to include diffusion measurements in contact treatments of different rock grain geometries (cube-cube, cube-sphere, and cube-tetrahedron) inside several RH (e.g., 43, 76, 93, 98, and nearly 100%) chambers controlled with saturated salt solutions. Different intergrain contact points will help us understand the role of pendular water elements and water film continuity in affecting/controlling diffusion pathways. Various RH conditions will be used to simulate the scenarios of transient RH environments inside the drifts following the emplacement of waste packages. It is likely that both water film thickness and continuity are closely related to RH conditions and hence to potential diffusive radionuclide transport.

2C. Column work:

(1). Half-cell experiments designed to both qualitatively (with dye) and quantitatively (various tracers with different aqueous diffusion coefficients) study diffusion will be used to examine gravel diffusion behavior in chambers with controlled high RH. This is analogous to no-seepage scenarios into the waste emplacement drifts, over 85% of the scenarios predicted by TSPA.

(2). Column tests are to be conducted from saturated to partially saturated conditions, with both nonsorbing (e.g., bromide) and sorbing (e.g., lithium, strontium, and cesium) tracers to examine advective-diffusive transport in invert materials. This is analogous to scenarios with seepage into drifts. The internal water in the gravel column is expected to behave as immobile water (i.e., not significantly participating in flow processes), while the surface water is expected to behave as mobile water, with its magnitude related to experimental fluxes. We will use the dual-continuum approach (i.e., mobile-immobile model) to describe solute transport behavior in the systems. The approach leads to a two-region advection-dispersion equation, with a first-order solute exchange process between the mobile and immobile regions (e.g., van Genuchten and Wierenga, 1976; Hu and Brusseau, 1995; Padilla et al., 1999). With numerical simulators to analyze resultant tracer breakthrough curves, two important parameters can be obtained. The first parameter, the mobile water fraction, provides us a quantification of mobile water (i.e., surface water in our systems); its value is expected to decrease as water content decreases. The second parameter, the mass-transfer coefficient

between the mobile and immobile water regions, characterizes nonequilibrium inter- and intra-porosity interaction. It relates to the interfacial area between these two regions, the volume and geometry of the immobile water, and the diffusion coefficients of the solutes.

3. Modeling:

   As the unique behavior of the invert system (containing both surface and internal water) is analogous to that of a fracture-matrix water system, we will adopt/expand the dual-continuum approach to model the unique characteristics of invert materials as a diffusion barrier. This will enable us to assess waste isolation performance as affected by flow and transport in the drift invert.

   Dual-diffusivity models will be constructed to account for the distinctly different diffusion processes along the rock surfaces and through the porous gravel. A dual-diffusivity model for crushed rocks is similar to a dual-permeability model for fractured rocks. The transitions from surface processes to bulk processes are governed by a surface-bulk interaction term. With data obtained in Phase 2 to calibrate the model, the model can be used to evaluate the uncertainties associated with diffusion processes, to refine invert design, and to assess invert performance. This model will be integrated with invert thermal-hydrologic and thermal-hydrologic-chemical models, because all current simulations consider only volume averaged property sets that do not incorporate nonequilibrium inter-and intra-porosity interaction.

Acknowledgments

This work was supported by the Director, Office of Civilian Radioactive Waste Management, U.S. Department of Energy, through Memorandum Purchase Order EA9013MC5X between Bechtel SAIC Company, LLC and the Ernest Orlando Lawrence Berkeley National Laboratory (Berkeley Lab). The support is provided to Berkeley Lab through the U.S. Department of Energy Contract No. DE-AC03-76SF00098. We greatly appreciate the help from Ingrid Zubieta for laboratory assistance, and Xiang-Lei Mao and Jhanis Gonzalez of Berkeley Lab for their insightful discussions and operation related to LA-ICP-MS. The authors also thank Yongkoo Seol, Lehua Pan, and Dan Hawkes of Berkeley Lab for many helpful comments.

References

Conca, J.L. 1990. Diffusion barrier transport properties of unsaturated Paintbrush tuff rubble backfill. *Proceedings of the First International High-Level Radioactive Waste Management Conference, 1:* 394–401.

Conca, J.L. and J. Wright. 1990. Diffusion coefficients in gravel under unsaturated conditions. *Water Resour. Res., 26*(5): 1055–1066.

Conca, J.L. and J. Wright. 1992. Diffusion and flow in gravel, soil, and whole rock. *Appl. Hydrogeo.,* 1: 5–24.

Crank, J. 1995. *The Mathematics of Diffusion*. 2nd ed., Oxford University Press, New York.

CRWMS M&O 2000. *Invert Diffusion Properties Model.* ANL-EBS-MD-000031 REV 01. Las Vegas, Nevada: CRWMS M&O. ACC: MOL.20000912.0208.

Cussler, E.L. 1984. *Diffusion: Mass Transfer in Fluid Systems*. Cambridge Univ. Press, New York.

Fityus S.G., D.W. Smith, and J.R. Booker. 1999. Contaminant transport through an unsaturated soil liner beneath a landfill. *Can Geotech. J.*, 36(2): 330–354.

Gee, M.L., T.W. Healy, and L.R. White. 1990. Hydrophobicity Effects in the Condensation of Water Films on Quartz. *J. Colloid Interface Sci.*, 140(2): 450–465.

Hu, Q., and M.L. Brusseau. 1995. Effect of solute size on transport in structured porous media. *Water Resour. Res.,* 31(7): 1637–1646.

Hu, Q., and J.S.Y. Wang. 2001. Diffusion in unsaturated geological media: A review. *Critical Reviews in Environmental Science and Technology* (submitted).

Johnson, J.W., K.G. Knauss, W.E. Glassley, L.D. DeLoach, and A.F.B. Thompson. 1998. Reactive transport modeling of plug-flow reactor experiments: quartz and tuff dissolution at 240^{o}C. *J. Hydrol.*, 209: 81–111.

Kozaki, T., K. Inada, S. Sato, and H. Ohashi. 2001. Diffusion mechanism of chloride ions in sodium montmorillonite. *J. Contam. Hydrol.*, 47: 159–170.

Nakashima, S. 1995. Diffusivity of ions in pore water as a quantitative basis for rock deformation rate estimates. *Tectonophysics*, 245(3-4): 185–203.

Olesen, T., P. Moldrup, K. Henriksen, and L.W. Petersen. 1996. Modeling diffusion and reactions in soils: IV. New models for predicting ion diffusivity. *Soil Sci.*, 161(10): 634–645.

Olesen, T., P. Moldrup, and J. Gamst. 1999. Solute diffusion and adsorption in six soils along a soil texture gradient. *Soil Sci. Soc. Am. J.*, 63: 519–524.

Padilla, I.Y., T.C.J. Yeh, and M.H. Conklin. 1999. The effect of water content on solute transport in unsaturated porous media. *Water Resour. Res.*, 35(11): 3303–3313.

Peterman, Z.E., and P.L. Cloke. 2001. Geochemical homogeneity of tuffs at the potential repository level, Yucca Mountain, Nevada: *Proceedings of the 9th International High-Level Radioactive Waste Management Conference (on CD)*.

Roberts, J.R., and W. Lin, 1997. Electrical properties of partially saturated Topopah Spring tuff: Water distribution as a function of saturation. *Water Resour. Res.*, 33(4): 577–587.

Rowell, D.L., M.W. Martin, and P.H. Nye. 1967. The measurement and mechanism of ion diffusion in soils. III. The effect of moisture content and soil-solution concentration on the self-diffusion of ions in soils. *J. Soil Sci.*, 18(2): 204–222.

Rundberg, R.S. 1987. Assessment report on the kinetics of radionuclide adsorption on Yucca Mountain tuff. Los Alamos National Laboratory. LA-11026-MS, New Mexico.

Russo, R.E., X.L. Mao, O.V. Borisov, and H.C. Liu. 2000. Laser ablation in atomic spectroscopy. *Encyclopedia of Analytical Chemistry: Instrumentation and Applications*. John Wiley & Sons.

Sawatsky, N.G., and D.W. Oscarson. 1991. Diffusion of technetium in dense under oxidizing and reducing conditions. *Soil Sci. Soc. Am. J.*, 55: 1261–1267.

Tokunaga, T. K., and J. Wan. 1997. Water film flow along fracture surfaces of porous rock. *Water Resour. Res.*, 33: 1287–1295.

Tokunaga, T.K., J. Wan, and S.R. Sutton. 2000. Transient film flow on rough fracture surfaces. *Water Resour. Res.*, *36*(7): 1737–1746.

Triay, I.R., A. Meijer, J.L. Conca, K.S. Kung, R.S. Rundberg, B.A. Strietelmeier, and C.D. Tait. 1997. Summary and synthesis report on radionuclide retardation for the Yucca Mountain Site Characterization Project Milestone 3784M, Los Alamos National Laboratory, Los Alamos.

van Genuchten, M.Th., and P.J. Wierenga. 1976. Mass transfer studies in sorbing porous media: 1. Analytical solutions. *Soil Sci. Soc. Am. J.*, 40(4): 473–480.

Wang, J.S.Y., E.L. Hardin, and L.D. Rickertsen. 2001. Crushed tuff as an invert diffusion barrier to enhance waste-isolation capacity. *Proceedings of the 9th International High-Level Radioactive Waste Management Conference* (on CD).